Supporting Information

Temperature dependence of charge separation and recombination in porphyrin oligomer-fullerene donor-acceptor systems

Axel Kahnt, [¤] *Joakim Kärnbratt,* [¤] *Louisa J. Esdaile,* [§] *Marie Hutin,* [§] *Katsutoshi Sawada,* [§] *Harry Anderson,* [§]* *Bo Albinsson*[¤]*

[¤]Department of Chemical and Biological Engineering

Physical Chemistry, Kemivägen 3, 412 96 Göteborg (Sweden)

Fax: (+46) 31-772-3858

[§]Department of Chemistry, University of Oxford

Chemistry Research Laboratory, Mansfield Road

Oxford OX1 3TA (UK)

Fax: (+44) 1865-275-704

balb@chalmers.se

harry.anderson@chem.ox.ac.uk

Table of Contents:

Section S1: **Synthetic Strategy and Schemes**

The sarcosine derivative **S1** was designed to overcome solubility problems with the longer fullerene-terminated porphyrin oligomers. It was synthesized in three steps from 3,5-dihydroxybenzaldehyde, as shown in Scheme S1.1.

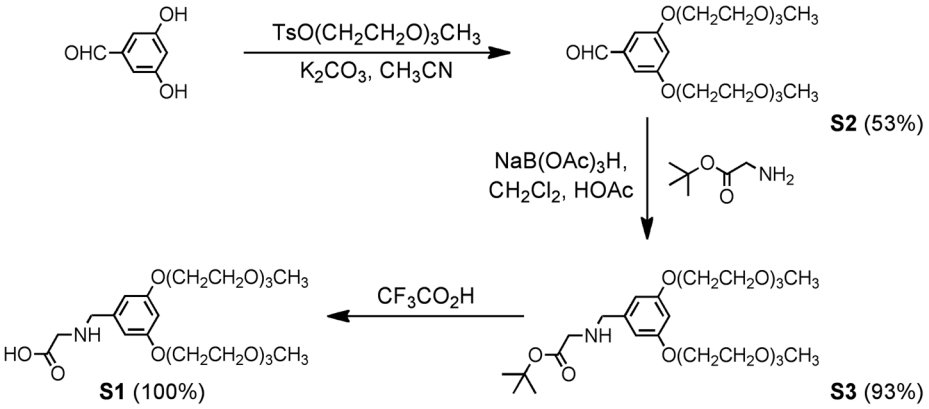

Scheme S1.1. The synthesis of sarcosine derivative **S1**.

The fullerene-terminated trimer and tetramer, $\mathbf{P_3}$-$\mathbf{C_{60}}$ and $\mathbf{P_4}$-$\mathbf{C_{60}}$, were prepared using Prato coupling, as shown in Scheme S1.2. The hexamer derivative $\mathbf{P_6}$-$\mathbf{C_{60}}$ was synthesized by the route shown in Scheme S1.3 which involves statistical cross-coupling of two trimers $\mathbf{P_3}$-**H** and **H**-$\mathbf{P_3}$-**CHO**.

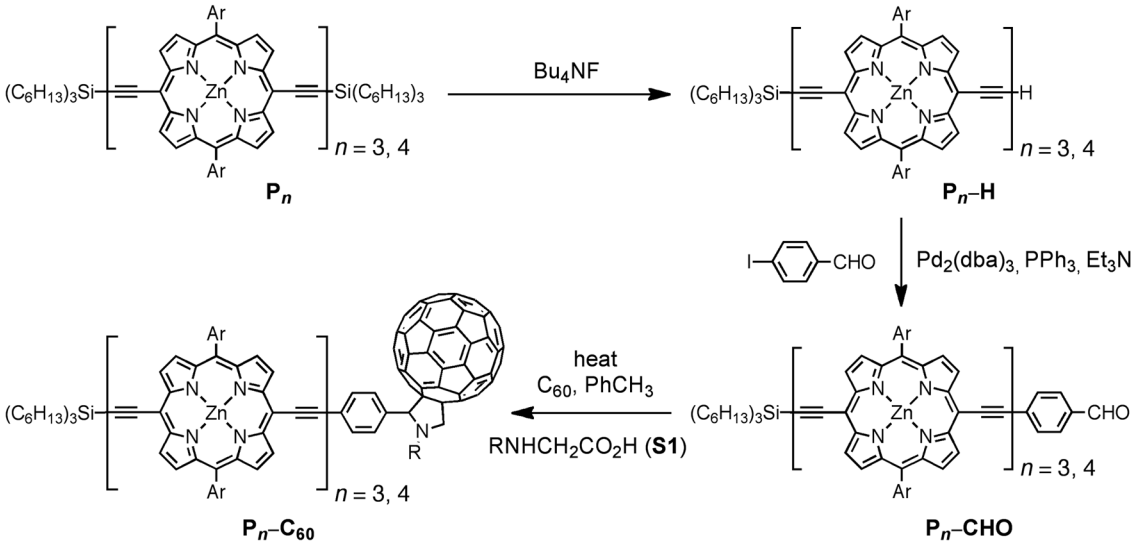

Scheme S1.2. The synthesis of fullerene-terminated porphyrin oligomers $\mathbf{P_3}$-$\mathbf{C_{60}}$ and $\mathbf{P_4}$-$\mathbf{C_{60}}$.

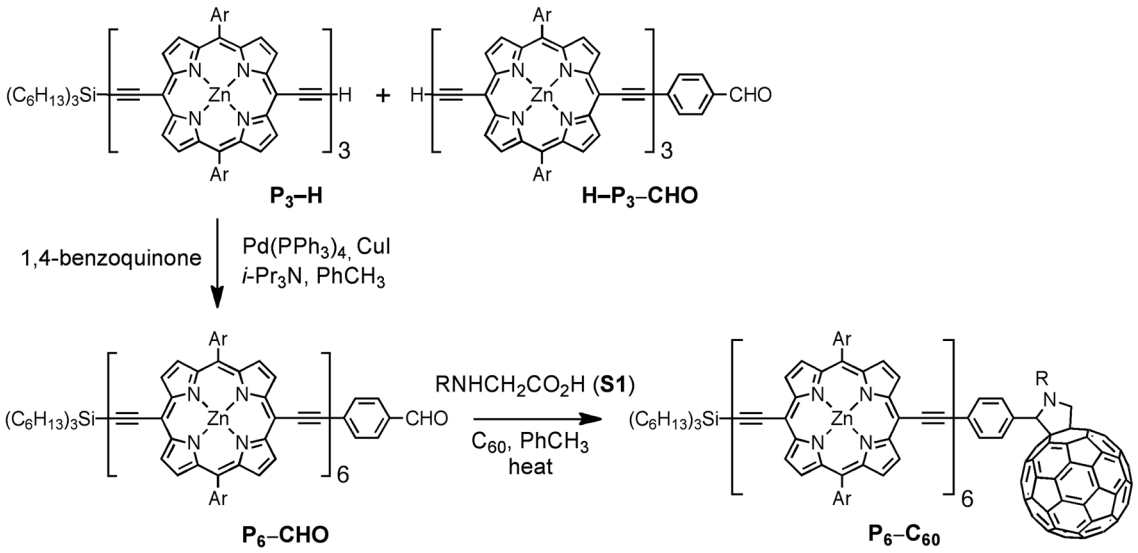

Scheme S1.3. The synthesis of hexamer $\mathbf{P_6\text{-}C_{60}}$.

Section S2: **Synthetic Procedures**

Materials, Instrumentation and General Synthetic Procedures. Solvents were dried by passing through alumina under N_2 pressure. Triethylamine was distilled from CaH_2. Manipulation of all air and/or water sensitive compounds was carried out using standard high vacuum techniques. Porphyrin oligomers $\mathbf{P_3}$, $\mathbf{P_4}$ and $\mathbf{P_4\text{-}CHO}$ were synthesized using published procedures.[1-2] Column chromatography was carried out on Merck® silica gel 60 using a positive pressure of nitrogen. TLC was carried out on aluminum backed silica gel 60 F254 plates. Size exclusion chromatography was carried out using Bio-Beads S-X1, 200–400 mesh (Bio-Rad). Where mixtures of solvents were used, ratios reported are by volume. NMR spectra were recorded on a Bruker DPX-400 spectrometer, unless otherwise stated. Chemical shifts are quoted as parts per million (ppm) relative to tetramethylsilane and coupling constants (*J*) are quoted in Hertz (Hz). MALDI-TOF mass spectra were acquired by the EPSRC Mass Spectrometry Service, Swansea, UK, using a DCTB matrix. UV-visible spectra were recorded on a Perkin-Elmer Lambda 20 spectrometer. HPLC purification was performed using HPLC grade solvents with an ACE column (dimensions 250 × 10 mm, 100 Å pore size, 5 μm phase silica) on a VWR-Hitachi LaChrom Elite system, equipped with an L-2455 Diode Array Detector, L-2200 Autosampler, L-2350 Column Oven, L-2130 Pump and a Foxy Jr. Fraction Collector.

Synthesis of 3,5-Bis(2-(2-(2-methoxyethoxy)ethoxy)ethoxy)benzaldehyde S2. 3,5-Dihydroxybenzaldehyde (0.50 g, 3.6 mmol) and K_2CO_3 (1.00 g, 7.7 mmol) were dried under

vacuum for 2 hr then acrylonitrile (3 cm^3) and triethyleneglycol monotosylate (2.3 g, 7.2 mmol) were added, and the mixture was heated to reflux under nitrogen for 16 hr. The solvent was removed and the product was purified by silica gel column chromatography (EtOAc, R_f = 0.3) to yield **S2** (827 mg, 53%) as a colorless liquid. ^{1}H NMR (400 MHz $CDCl_3$): δ = 9.89 (s, 1H), 7.03 (d, J = 2.2, 2H), 6.77 (t, J = 2.3, 1H), 4.18 (t, J = 4.4, 4H), 3.89 (t, J = 5.0, 4H), 3.75–3.55 (m, 16H), 3.39 (s, 6H) (This compound has been prepared previously using similar procedures).[3-5]

Synthesis of Aryl-sarcosine *tert*-Butyl ester S3. 3,5-Bis(2-(2-(2-methoxyethoxy)ethoxy)ethoxy)benzaldehyde **S2** (650 mg, 1.51 mmol) was dissolved in CH_2Cl_2 (64 cm^3) under argon and acetic acid was added (1.28 cm^3). Glycine *tert*-butyl ester (2 eq., 413 µl, 3.02 mmol) was added, the mixture was stirred for 20 min, sodium triacetoxyborohydride (2.5 eq., 801 mg, 3.78 mmol) was then added and the mixture was stirred for a further 1 hr. A saturated aqueous solution of sodium carbonate (25 cm^3) was then added, the product extracted in to CH_2Cl_2 (3 × 20 cm^3), the organic layer washed with brine (25 cm^3), dried ($MgSO_4$), filtered and the solvent removed to give **S3** as a pale yellow oil (765 mg, 93 %). ^{1}H NMR (400 MHz $CDCl_3$): δ = 6.50 (d, J = 2.2, 2H, ArH), 6.40 (t, J = 2.2, 1H, ArH), 4.10 (t, J = 4.7, 4H, OCH_2), 3.86–3.83 (m, 4H, OCH_2), 3.76–3.72 (m, 6H, 4 OCH_2, 2 CH_2) 3.70–3.65 (m, 8H, OCH_2), 3.58–3.55 (m, 4H, OCH_2), 3.39 (s, 6H, OCH_3), 3.28 (s, 2H, CH_2), 1.47 (s, 9H, OCH_3); *m/z* (ESI) 546.3 [$(M + 1)^+$ $C_{27}H_{48}NO_{10}$ calc. 546.3], 489.3 [$(M - {}^tBu)^+$ $C_{23}H_{39}NO_{10}$ calc. 489.3].

Synthesis of Aryl-sarcosine S1. Aryl-sarcosine *tert*-butyl ester **S3** (202 mg, 0.307 mmol) was dissolved in trifluoroacetic acid (11 eq., 0.409 mmol, 2.75 cm^3) and the solution was stirred for 1 hr. The solvent was removed, the product dissolved in water (2 cm^3) and neutralized with sodium hydroxide solution (1.0 M) to pH 7 and the solvent removed. The resulting residue was dissolved in CH_2Cl_2 (20 cm^3), filtered and the solvent removed and the resulting pale yellow oil (245 mg, quant.) was dried under vacuum. ^{1}H NMR (400 MHz $CDCl_3$): δ = 6.61 (d, J = 2.0, 2H, ArH), 6.44 (t, J = 2.0, 1H, ArH), 4.07–4.04 (m, 4H, OCH_2), 3.93 (br, 2H, CH_2), 3.81–3.78 (m, 4H, OCH_2), 3.71–3.68 (m, 4H, OCH_2) 3.66–3.60 (m, 8H, OCH_2), 3.53–3.50 (m, 4H, OCH_2), 3.37 (br, 2H, CH_2), 3.31 (s, 6H, OCH_3); *m/z* (ESI) 490.3 [$(M + 1)^+$ $C_{23}H_{40}NO_{10}$ calc. 490.3], 512.2 [$(M + Na)^+$ $C_{23}H_{39}NNaO_{10}$ calc. 512.2].

Synthesis of P_3-CHO. The protected porphyrin trimer **P_3** (50.9 mg, 0.0132 mmol) was dissolved in dry CH_2Cl_2 (1.6 cm^3) and $CHCl_3$ (1.6 cm^3). TBAF solution (1.0 M in THF, 1.5 eq., 0.027 mmol, 27 µl) was added and the mixture was stirred under argon for 23 min, monitored by TLC [40–60 petroleum ether/pyridine (85:15)]. Acetic acid (50 µl, 0.87 mmol) was added, the mixture was passed though a short column of silica (CH_2Cl_2) and the solvent was removed. This mixture was used immediately in the next step without further purification. Deprotected trimer mixture (0.0132 mmol), *para*-iodobenzaldehyde (10 eq., 0.133 mmol, 30.9 mg), $Pd_2(dba)_3$ (10 mol%, 0.0013 mmol, 1.2 mg) and PPh_3 (40 mol%, 0.0053 mmol, 1.4 mg) were dried under vacuum for 40 min, and the vessel was purged with argon. Triethylamine (4.3 cm^3) was added, the mixture was treated to three freeze-pump-thaw cycles and then heated to 50 °C under argon for 14 hr. The mixture was passed though a short column of silica (CH_2Cl_2), the solvent removed and the residue was separated using column chromatography with 40–60 petroleum ether/pyridine (85:15) as eluent. The first eluting band was unreacted **P_3**, followed by the desired product **P_3-CHO**. The product was purified by recrystallization from CH_2Cl_2/MeOH to give a dark brown powder (17.6 mg, 36 % over 2 steps). ^{1}H NMR (400 MHz $CDCl_3$ / 1 % C_5D_5N): δ = 10.15 (s, 1H, CHO_a), 9.89–9.86 (m, 8H, $\beta H_{b2\text{-}5}$), 9.70 (d, J = 4.4, 2H, βH_{b1}), 9.64 (d, J = 4.6, 2H, βH_{b6}), 9.08–9.06 (m, 8H, $\beta H_{c2\text{-}5}$), 9.03 (d, J = 4.4, 2H, βH_{c1}), 8.97 (d, J = 4.6, 2H, βH_{c6}), 8.18 (d, J = 8.0, 2H, ArH_d), 8.09 (d, J = 8.0, 2H, ArH_e), 7.42 (d, J = 2.2, 4H, ArH_{f2}), 7.39 (d, J = 2.0, 4H, ArH_{f1}), 7.38 (d, J = 2.2, 4H, ArH_{f3}), 6.93–6.91 (m, 6H, ArH_g), 4.19–4.16 (m, 24H, octyl-CH_{2h}), 1.95–1.89 (m, 24H, octyl-CH_{2h}), 1.83–1.75 (m, 6H, hexyl-CH_{2i}), 1.59–1.52 (m, 36 H, 12 hexyl-CH_{2i}, 24 octyl-CH_{2h}), 1.42–1.28 (m, 102H, 6 hexyl-CH_{2i}, 96 octyl-CH_{2h}), 1.06–1.02 (m, 6H, hexyl-CH_{2i}), 0.95–0.86 (m, 45H, 9 hexyl-CH_{3i}, 36 octyl-CH_{3h}); *m/z* (MALDI) 3643.0 (M^+, $C_{229}H_{290}N_{12}O_{13}SiZn_3$ calc. 3643.0); UV/vis ($CHCl_3$/pyridine 99:1): λ_{max}/nm ($\varepsilon/10^3$ M^{-1} cm^{-1}) 468 (523), 500 (227), 590 (29.0), 699 (sh 93.4), 759 (181); UV/vis (THF): λ_{max}/nm ($\varepsilon/10^3$ M^{-1} cm^{-1}) 464 (556), 496 (237), 585 (32.1), 697 (sh 111), 743 (175); UV/vis (THF/pyridine 99:1): λ_{max}/nm ($\varepsilon/10^3$ M^{-1} cm^{-1}) 466 (567), 497 (224), 589 (30.5), 698 (sh 106), 749 (174).

Synthesis of P_3-C_{60}. C_{60} (10 eq., 0.0274 mmol, 19.7 mg) was sonicated in dry toluene (6.7 cm^3) for 1 hr and this solution was added to vacuum-dried **P_3-CHO** (10.0 mg, 0.00274 mmol) and

aryl-sarcosine **S1** (20 eq., 0.0549 mmol, 26.9 mg). The mixture was degassed and refluxed under argon for 13 hr, then allowed to cool, purified on silica (toluene, then CH_2Cl_2, then CH_2Cl_2/MeOH 1 %) and recrystallized from CH_2Cl_2/MeOH to give **P_3-C_{60}** as a dark brown powder (10.6 mg, 81 %). ^{1}H NMR (400 MHz $CDCl_3$ / 1 % C_5D_5N): δ = 9.88–9.86 (m, 8H, $\beta H_{a2\text{-}5}$), 9.71 (d, J = 4.4, 2H, βH_{a1}), 9.64 (d, J = 4.4, 2H, βH_{a2}), 9.07–9.05 (m, 8H, $\beta H_{b2\text{-}5}$), 8.98 (d, J = 4.6, 2H, βH_{b1}), 8.97 (d, J = 4.6, 2H, βH_{b6}), 8.12 (br, 4H, ArH_c), 7.41 (d, J = 2.0, 4H, ArH_{d2}), 7.39 (m, 8H, $ArH_{d1,3}$), 6.94–6.91 (m, 8H, 6 ArH_e, 2 ArH_f), 6.58–6.57 (m, 1H, ArH_g), 5.29 (br, 1H, CH_h), 4.94–4.91 (m, 1H, CH_{2i}), 4.65–4.60 (br, 1H, CH_{2j}), 4.26–4.24 (m, 4H, OCH_{2k}), 4.20–4.16 (m, 25H, 24 octyl-CH_{2l}, 1 CH_{2i}), 3.95–3.93 (m, 4H, OCH_{2k}), 3.80–3.78 (m, 4H, OCH_{2k}), 3.73–3.71 (m, 4H, OCH_{2k}), 3.68–3.66 (m, 5H, 4 OCH_{2k}, 1 CH_{2j}), 3.57–3.55 (m, 4H, OCH_{2k}), 3.38 (s, 6H, OCH_{3m}), 1.93–1.75 (m, 36H, 24 octyl-CH_{2l}, 6 hexyl-CH_{2n}), 1.58–1.51 (m, 36H, 12 hexyl-CH_{2n}, 24 octyl-CH_{2l}), 1.41–1.26 (m, 102H, 6 hexyl-CH_{2n}, 96 octyl-CH_{2l}), 1.06–1.00 (m, 6H, hexyl-CH_{2n}), 0.93–0.85 (m, 45H, 9 hexyl-CH_{3n}, 36 octyl-CH_{3l}); *m/z* (MALDI) 3791.3 (M^+, $C_{311}H_{327}N_{13}O_{20}SiZn_3$ calc. 3791.3); UV/vis ($CHCl_3$/pyridine 99:1): λ_{max}/nm ($\varepsilon/10^3$ M^{-1} cm^{-1}) 466 (505), 500 (215), 590 (29.6), 699 (sh 88.4), 759 (172); UV/vis (THF): λ_{max}/nm ($\varepsilon/10^3$ M^{-1} cm^{-1}) 462 (535), 496 (228), 586 (31.3), 688 (sh 101), 743 (167); UV/vis (THF/pyridine 99:1): λ_{max}/nm ($\varepsilon/10^3$ M^{-1} cm^{-1}) 465 (554), 498 (218), 587 (30.7), 698 (sh 103), 749 (168). Nierengarten and co-workers studied the restricted rotation of aryl-substituted fullerene derivatives.[6] Our spectral assignment around the C_{60} group is in agreement with that reported.

Synthesis of P_4-C_{60}. C_{60} (0.0226 mmol, 16.3 mg) was sonicated in dry toluene (10 cm^3) for 1 hr and this solution was added to vacuum-dried **P_4-CHO** (21.4 mg, 0.00453 mmol) and aryl-sarcosine **S1** (0.0453 mmol, 22.2 mg). The mixture was degassed and refluxed under nitrogen overnight.

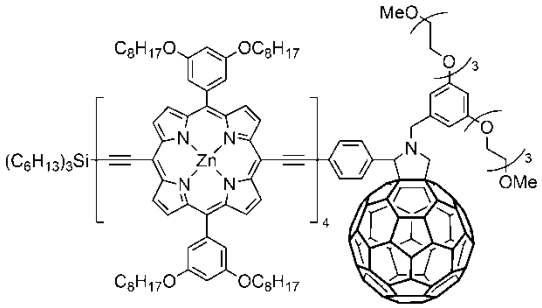

The mixture was allowed to cool, purified on silica (toluene, then CH_2Cl_2, then CH_2Cl_2/MeOH 1 %) and then recrystallized from CH_2Cl_2/MeOH to give **P_4-C_{60}** as a dark brown powder (25.2 mg, 94 %). ^{1}H NMR (250 MHz $CDCl_3$ / 1 % C_5D_5N, 298K): δ = 9.86–9.89 (m, 12H, $\beta H_{a2\text{-}7}$), 9.70 (d, J = 4.5, 2H, βH_{a1}), 9.64 (d, J = 4.5, 2H, βH_{a8}), 9.08–9.04 (m, 12H, $\beta H_{b2\text{-}7}$), 8.97 (d, J = 4.5, 2H, βH_{b1}), 8.96 (d, J = 4.5, 2H, βH_{b8}), 8.12 (br, 4H, ArH_c), 7.41 (d, J = 2, 8H, $ArH_{d2\text{-}3}$), 7.37 (m, 8H, $ArH_{d1,4}$), 6.94–6.91 (m, 10H, 8 ArH_e, 2 ArH_f), 6.67 (br, 1H, ArH_g), 5.13 (br, 1H, CH_h), 4.92 (br, 1H, CH_{2i}), 4.60 (br, 1H, CH_{2j}), 4.21–4.14 (m, 37H, 4 CH_{2k}, 32 octyl-CH_{2l}, 1 CH_{2i}), 3.96–3.92 (m, 4H, OCH_{2k}), 3.81–3.77 (m, 4H, OCH_{2k}), 3.74–3.71 (m, 4H, OCH_{2k}), 3.68–3.64 (m, 5H, 4 OCH_{2k}, 1 CH_{2j}), 3.57–3.53 (m, 4H, OCH_{2k}), 3.37 (s, 6H, OCH_{3m}), 1.93–184 (m, 32H, octyl-CH_{2l}), 1.80–1.72 (m, 6H, hexyl-CH_{2n}), 1.59–1.48 (m, 44H, 12 hexyl–CH_{2n}, 32 octyl-CH_{2l}), 1.42–1.25 (m, 150H, 6 hexyl-CH_{2n}, 144 octyl-CH_{2l}), 1.06–0.99 (m, 6H, hexyl-CH_{2n}), 0.93–0.83 (m, 63H, 9 hexyl-CH_{3n}, 54 octyl-CH_{3l}); *m/z* (MALDI + NaOAc) 5877.4 (M^+, $C_{379}H_{409}N_{17}O_{24}SiZn_4$ calc. 5876.05), 5211.3 ([M – C_{60} + AcO^-]$^+$, calc. 5216.8; UV/vis ($CHCl_3$/pyridine 99:1): λ_{max}/nm (ε/10^3 M^{-1} cm^{-1}) 467 (511), 769 (210).

Synthesis of P_6-C_{60}. The protected porphyrin trimer **P_3** (49.6 mg, 0.0130 mmol) was dissolved in dry CH_2Cl_2 (1.6 cm^3) and $CHCl_3$ (1.6 cm^3) and mixture was placed under argon. TBAF solution (1.0 M in THF, 2 eq., 0.026 mmol, 26 µl) was added and the mixture was stirred under

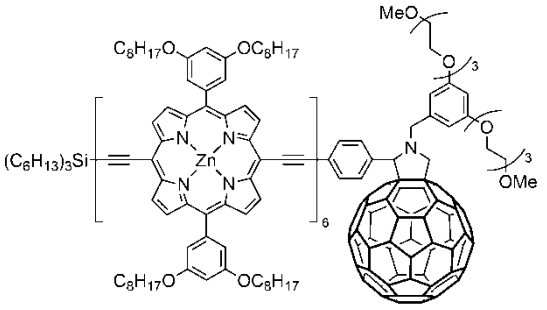

argon for 35 min, monitored by TLC (40–60 petroleum ether/pyridine/THF 85:10:5). The mixture was passed though a short column of silica (CH_2Cl_2) and the solvent was removed. The residue was separated using column chromatography with 40–60 petroleum ether/pyridine (85:15) as eluent. The first eluting band was unreacted **P_3** (29.2 mg, 59 %), followed by the desired intermediate **P_3-H** (14.1 mg, 31 %).

P_3-CHO (14.5 mg, 0.00398 mmol) was dissolved in CH_2Cl_2 (2 cm^3) under argon, TBAF solution (1.0 M in THF, 10 eq., 0.0398 mmol, 40 µl) was added and the mixture was stirred at

room temperature for 30 min. Mixture was passed through a short column of silica (CH_2Cl_2/pyridine 99:1) to give the desired **H-P$_3$-CHO**, and this product was used immediately in the next step without further purification.

P$_3$-H (14.1 mg, 0.00398 mmol), **H-P$_3$-CHO** (0.00398 mmol), $Pd(PPh_3)_4$ (5 mol%, 0.000398 mmol, 0.46 mg), CuI (50 mol%, 0.00398 mmol, 0.76 mg) and 1,4-benzoquinone (2 eq., 0.0159 mmol, 1.7 mg) were dried for 25 min, the vessel was purged with argon. Diisopropylamine (0.77 cm^3) and toluene (2.0 cm^3) were added and the mixture was heated to 50 °C for 15 hr. The statistical mixture was passed through a short silica column (CH_2Cl_2/pyridine 99:1), and purified by size exclusion chromatography (toluene with 0.02 % pyridine). C_{60} (10 eq., 0.0332 mmol, 23.9 mg) was sonicated in dry toluene (11 cm^3) and pyridine (1%, 110 μl) for 30 min and this solution was added to vacuum-dried hexamer mixture (22.9 mg, 0.00332 mmol) and aryl-sarcosine **S1** (20 eq., 0.0664 mmol, 32.5 mg). The mixture was degassed, refluxed under argon for 15 hr and allowed to cool. The mixture was purified using a silica chromatography (toluene/pyridine 99:1, then toluene/THF/pyridine 97:2:1, then toluene/THF/pyridine 89:10:1). The first eluting band was **P$_6$**, followed by the desired product **P$_6$-C$_{60}$**. This fraction was purified using semi-preparative HPLC, and the product was then recrystallized from CH_2Cl_2/MeOH to give a dark brown powder (**P$_6$-C$_{60}$**, 4.1 mg, 15 %, from 3 steps). ^{1}H NMR (400 MHz $CDCl_3$ / 1 % C_5D_5N): δ = 9.90–9.87 (m, 20H, $\beta H_{a2\text{-}11}$), 9.71 (d, J = 4.4, 2H, βH_{a1}), 9.64 (d, J = 4.5, 2H, βH_{a12}), 9.09–9.07 (m, 20H, $\beta H_{b2\text{-}11}$), 8.98 (d, J = 4.4, 2H, βH_{b1}), 8.96 (d, J = 4.5, 2H, βH_{b12}), 8.13 (br, 4H, ArH_c), 7.44–7.42 (m, 16H, $ArH_{d2\text{-}5}$), 7.39–7.37 (m, 8H, $ArH_{d1,6}$) 6.95–6.91 (m, 14H, 12 ArH_e, 2 ArH_f), 6.58–6.57 (m, 1H, ArH_g), 5.28 (br, 1H, CH_h), 4.92–4.89 (m, 1H, CH_{2i}), 4.65–4.60 (br, 1H, CH_{2j}), 4.32–4.08 (m, 53H, 4 OCH_{2k}, 48 octyl-CH_{2l}, 1 CH_{2i}), 3.94–3.91 (m, 4H, OCH_{2k}), 3.79–3.76 (m, 4H, OCH_{2k}), 3.73–3.70 (m, 4H, OCH_{2k}), 3.68–3.65 (m, 5H, 4 OCH_{2k}, 1 CH_{2j}), 3.57–3.54 (m, 4H, OCH_{2k}), 3.37 (s, 6H, OCH_{3m}), 1.94–1.75 (m, 54H, 48 octyl-CH_{2l}, 6 hexyl-CH_{2n}), 1.59–1.50 (m, 60H, 12 hexyl-CH_{2n}, 48 octyl-CH_{2l}), 1.44–1.25 (m, 198H, 6 hexyl-CH_{2n}, 192 octyl-CH_{2l}), 1.05–1.00 (m, 6H, hexyl-CH_{2n}), 0.94–0.84 (m, 81H, 9 hexyl-CH_{3n}, 72 octyl-CH_{3l}); UV/vis ($CHCl_3$/pyridine 99:1): λ_{max}/nm ($\varepsilon/10^3$ M^{-1} cm^{-1}) 468 (666), 500 (sh 445), 592 (48.8), 795 (299); UV/vis (THF): λ_{max}/nm ($\varepsilon/10^3$ M^{-1} cm^{-1}) 465 (724), 495 (466), 587 (52.1), 766 (305); UV/vis ($CHCl_3$/pyridine 99:1): λ_{max}/nm ($\varepsilon/10^3$ M^{-1} cm^{-1}) 466 (737), 497 (sh 450), 589 (50.7), 776 (307).

Section S3: **NMR Spectra**

P_3-CHO; ^{1}H NMR (400 MHz, $CDCl_3$/1 % C_5H_5N)

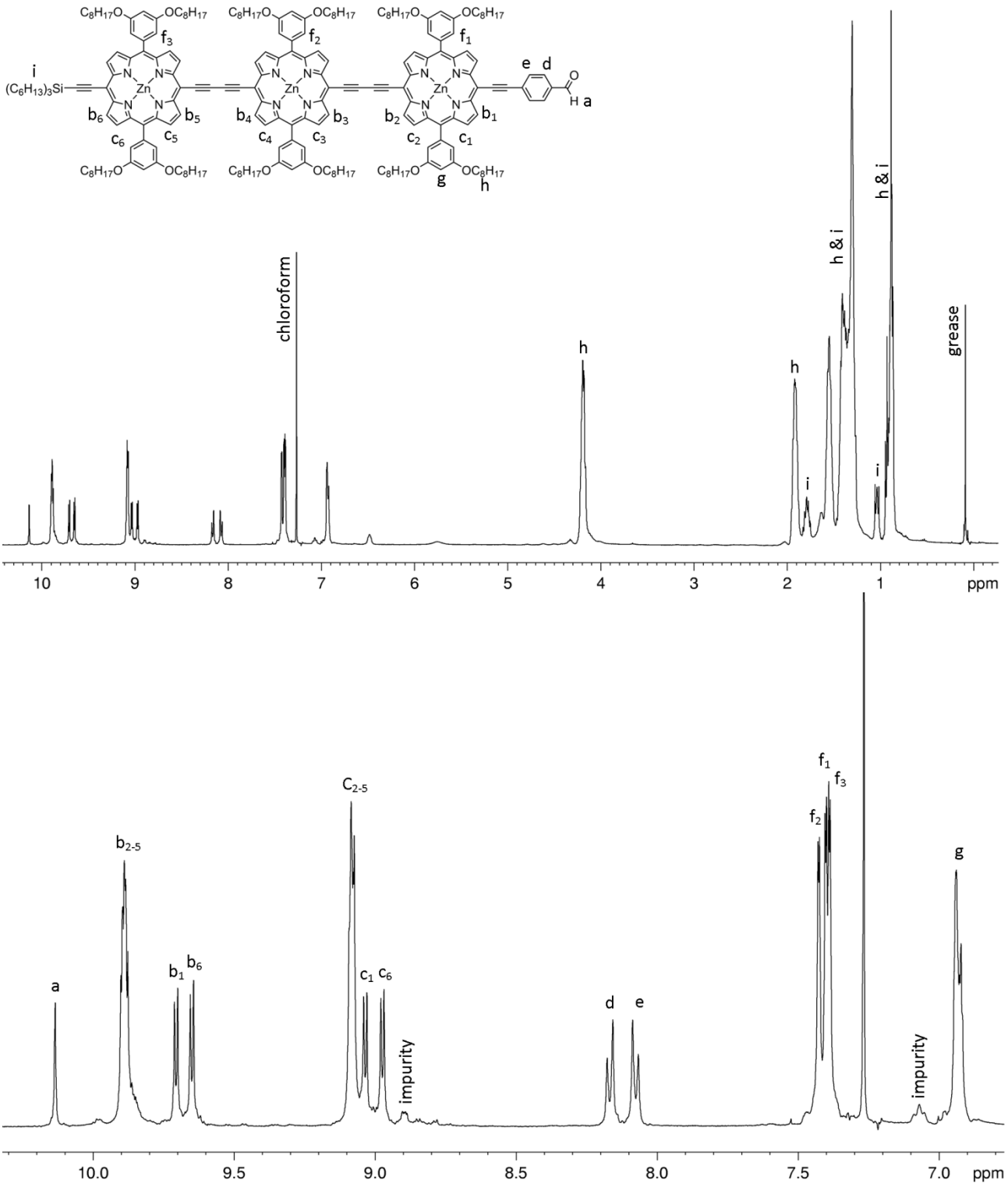

P_3-C_{60}; ^{1}H NMR (400 MHz, $CDCl_3$/1 % C_5H_5N)

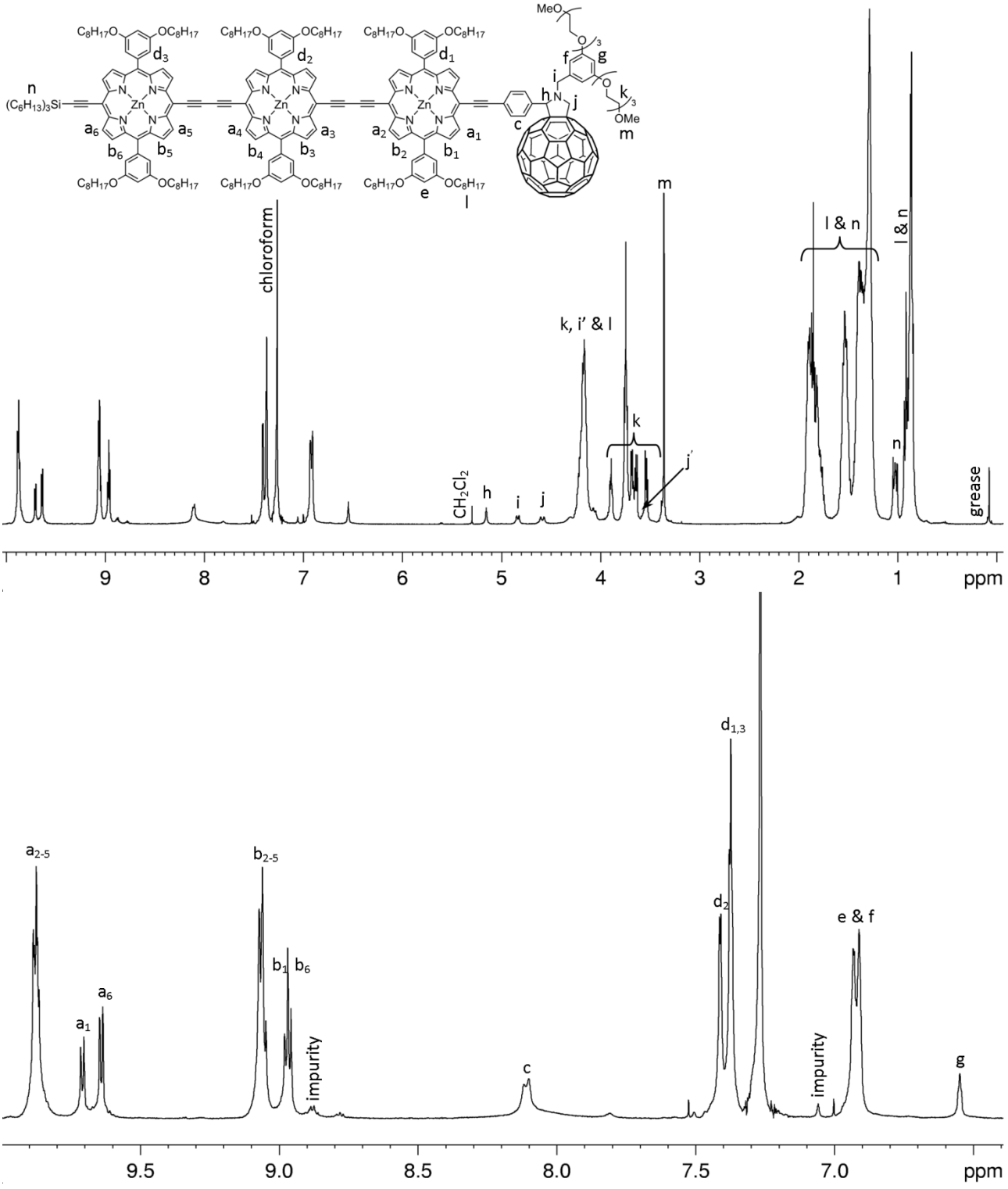

P_4-C_{60}; ^{1}H NMR (250 MHz, $CDCl_3$/1 % C_5H_5N)

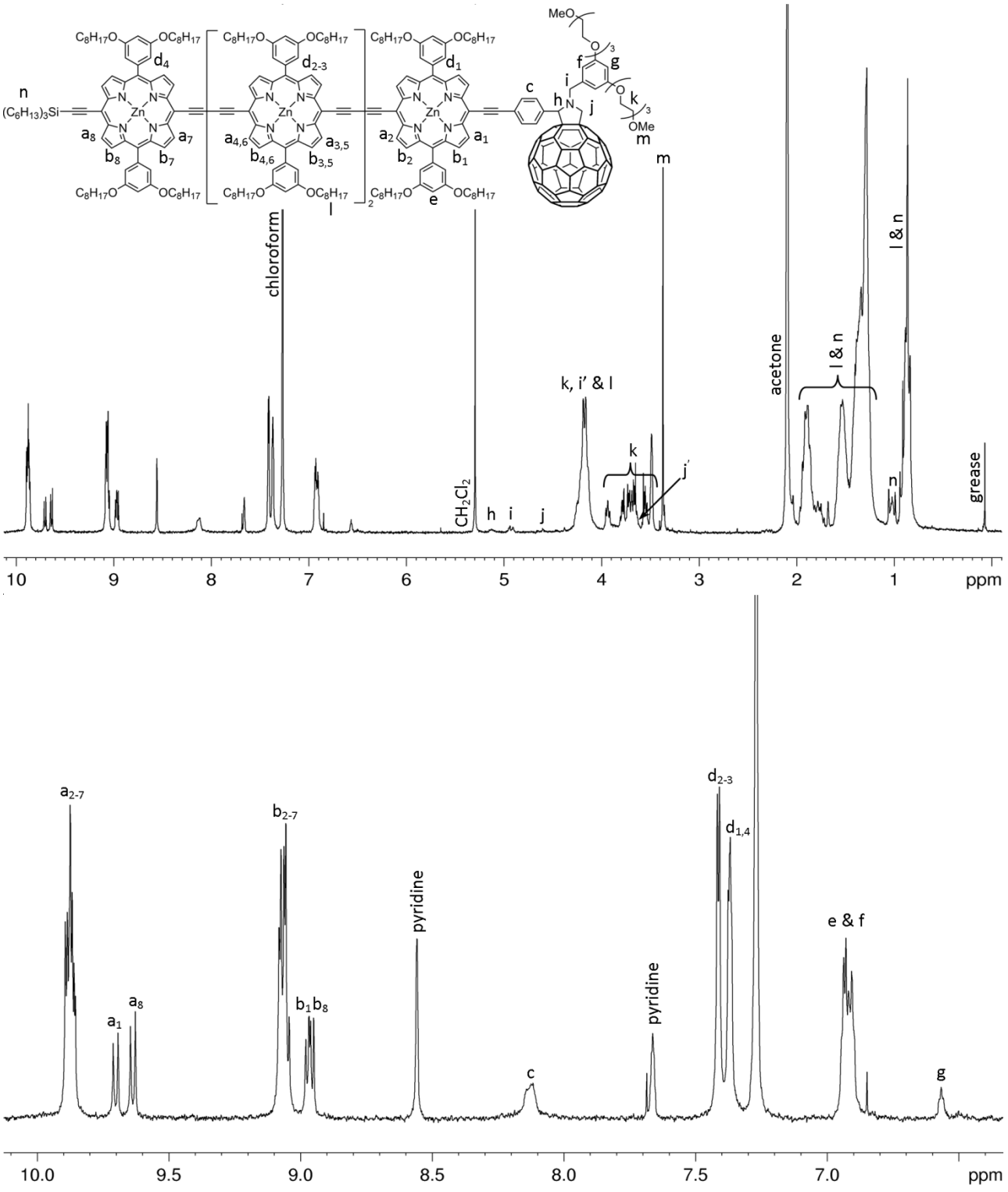

P_6-C_{60}; ^{1}H NMR (400 MHz, $CDCl_3$/1 % C_5H_5N)

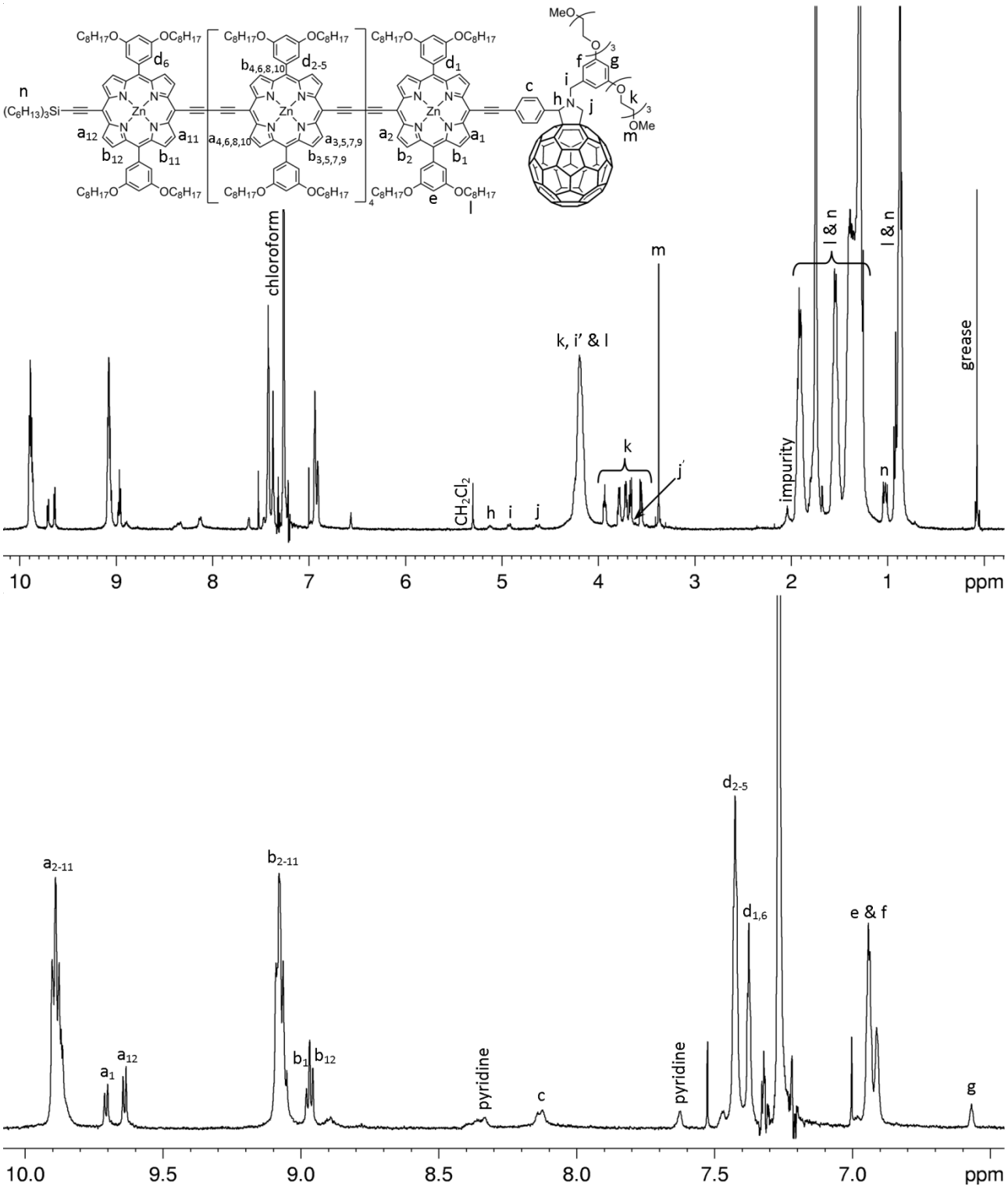

Section S4: **Mass Spectra**

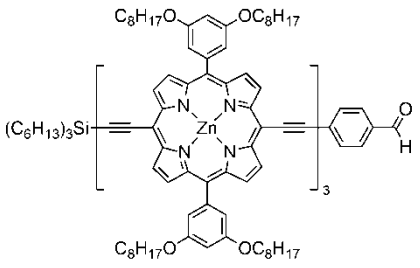

P_3-CHO:

Matrix: DCTB

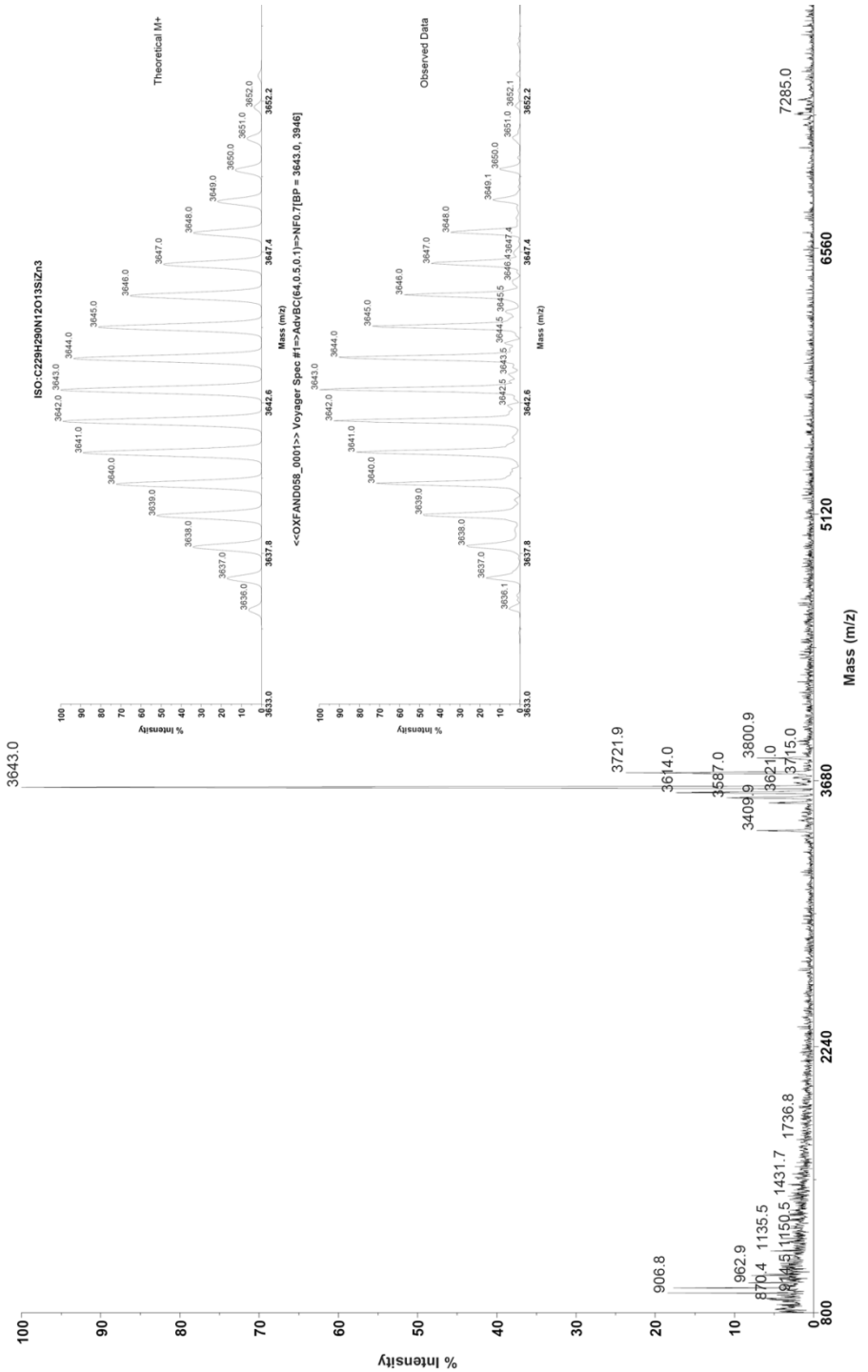

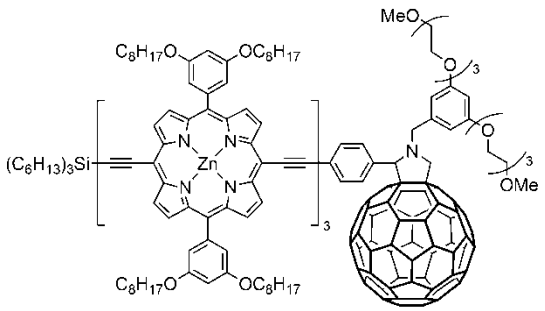

P_3-C_{60}:

Matrix: DCTB

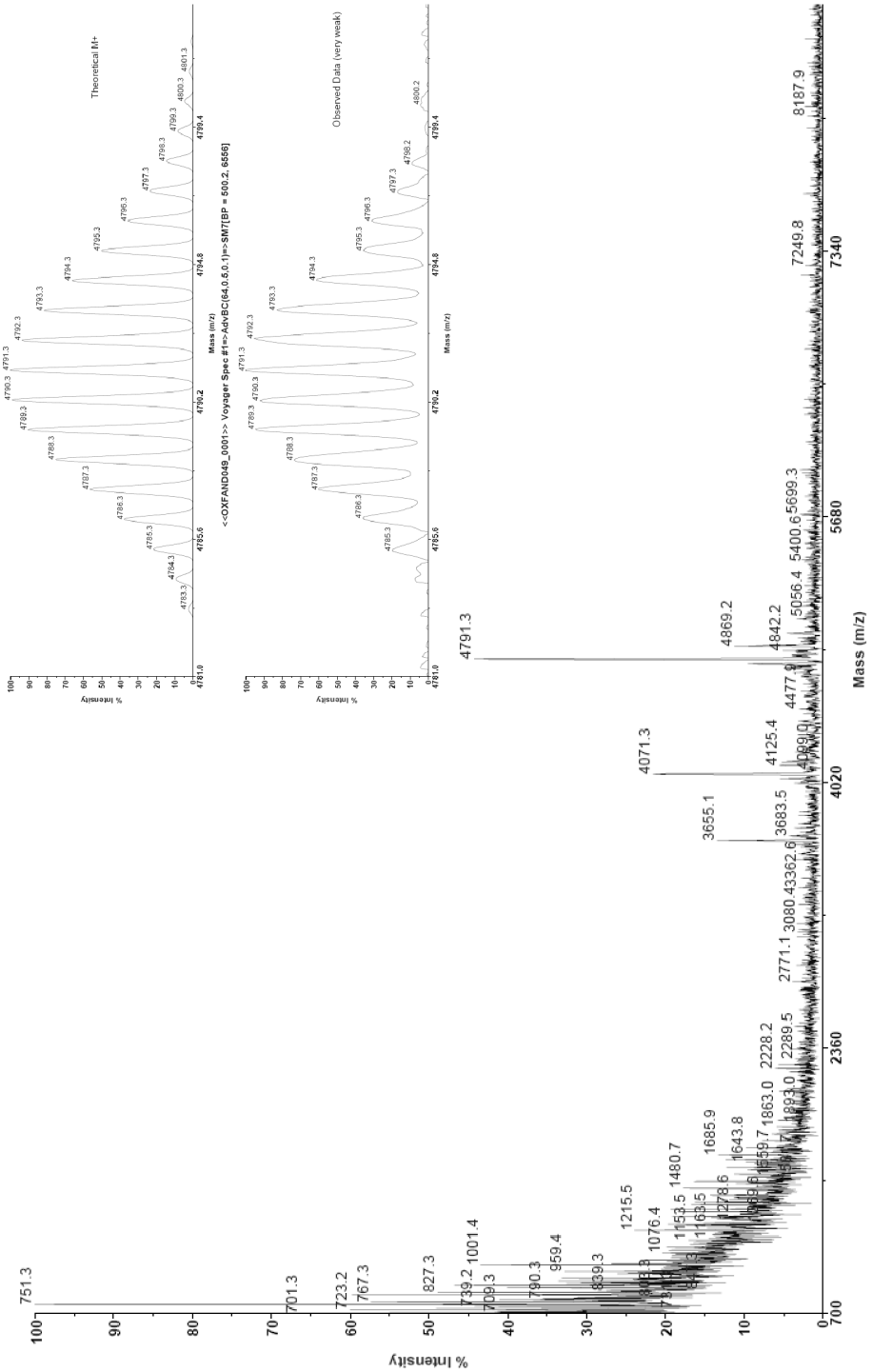

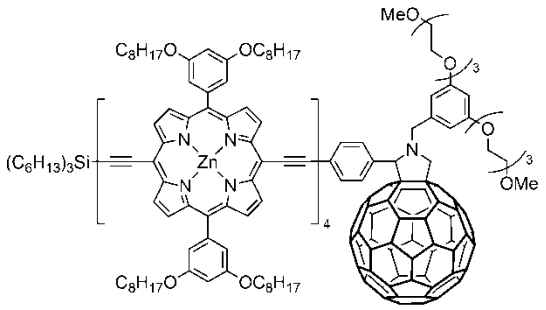

P_4-C_{60}:

Matrix: DCTB

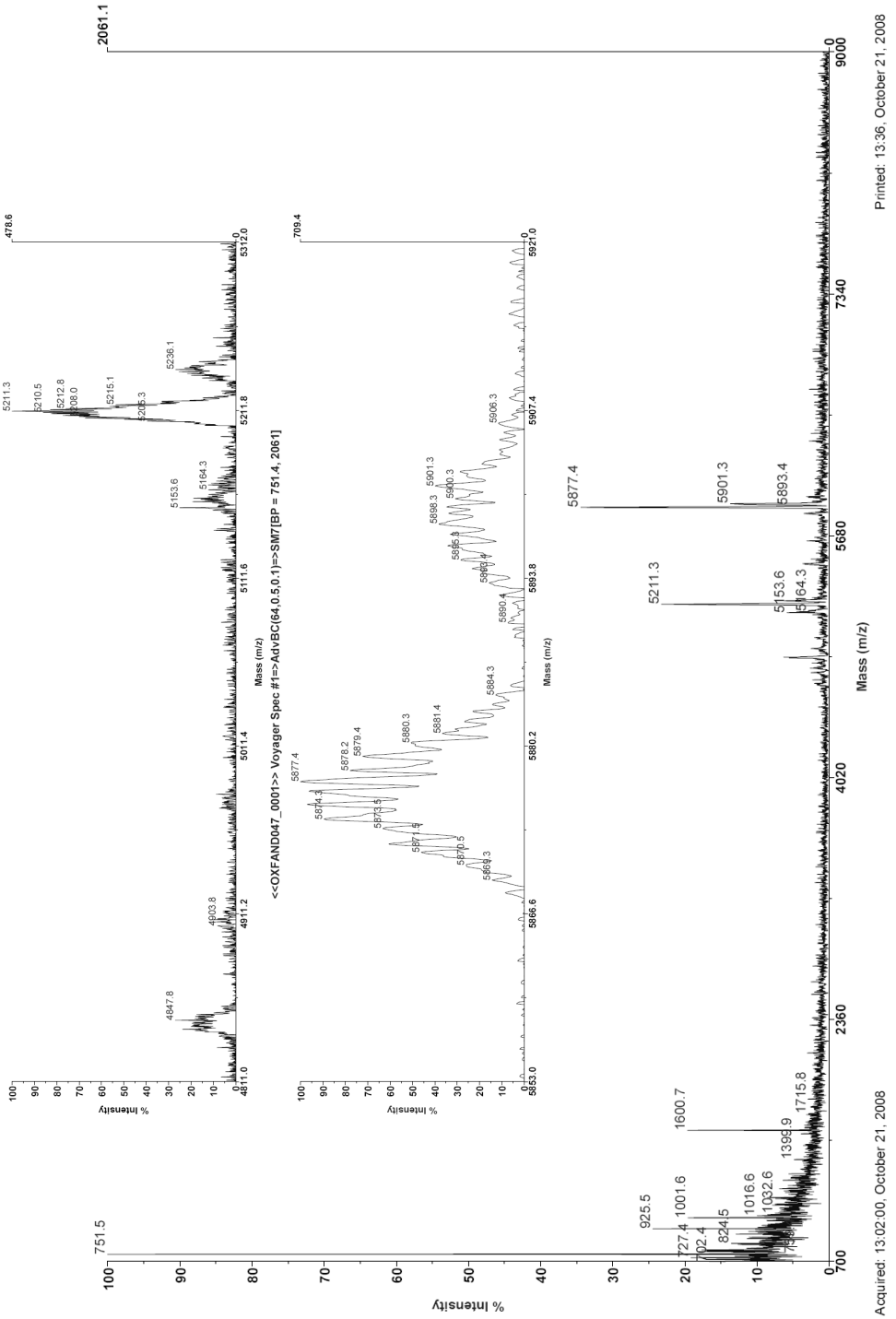

Section S5: **HPLC traces**

The HPLC purification of compounds **P3-C60**, **P4-C60** and **P6-C60** was performed using a flow rate of 4 mL/min with the following method:

Time (min)	% Toluene (with 1% pyridine)	% THF
0	80	20
8	65	35
9	35	65
10	80	20
14	80	20

P_3-C_{60}

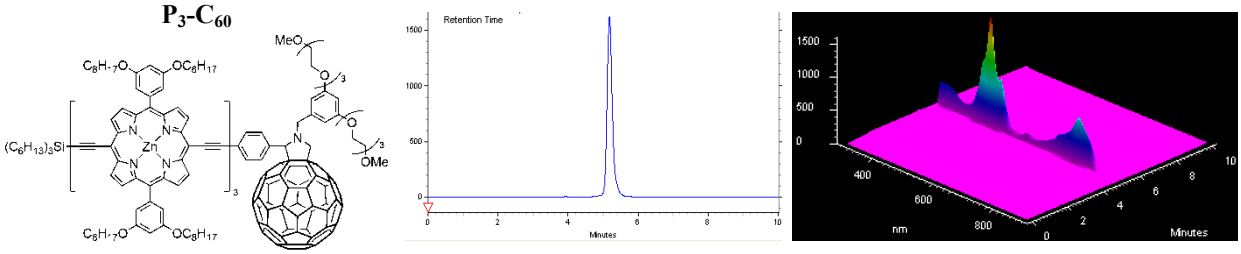

P_4-C_{60}

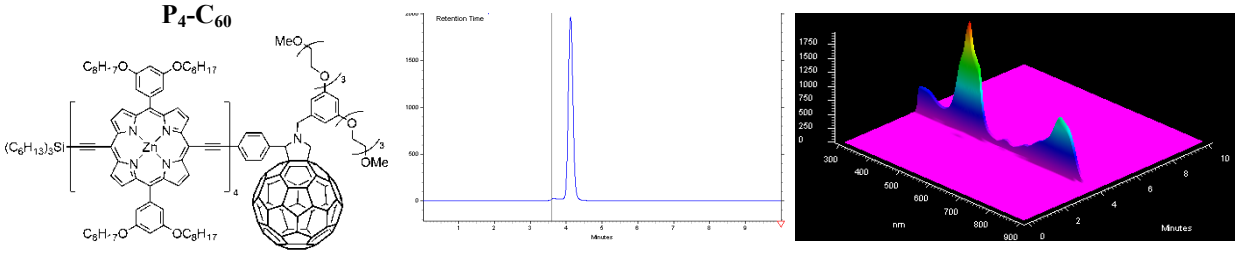

P_6-C_{60}

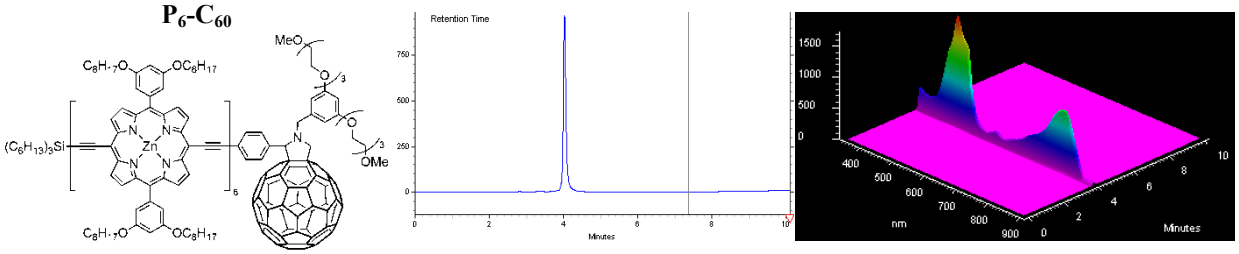

Section S6: **UV/ vis absorption spectra of the oligoporphyrin-fullerene compounds at different temperatures**

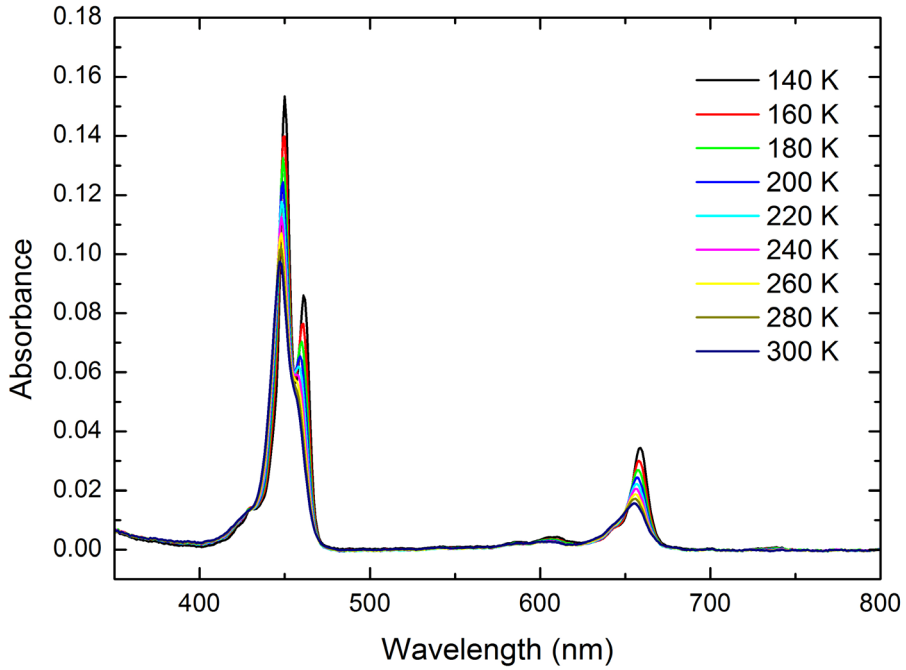

Figure S6.1. Ground state absorption of $\mathbf{P_1}$-$\mathbf{C_{60}}$ in 2MTHF + 1% pyridine at different temperatures.

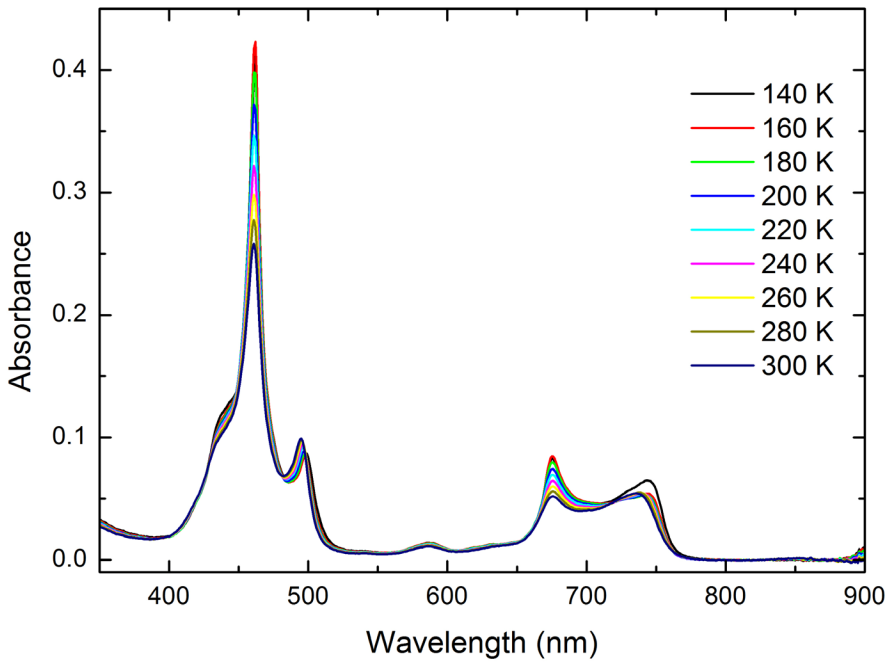

Figure S6.2. Ground state absorption of $\mathbf{P_2}$-$\mathbf{C_{60}}$ in 2MTHF + 1% pyridine at different temperatures.

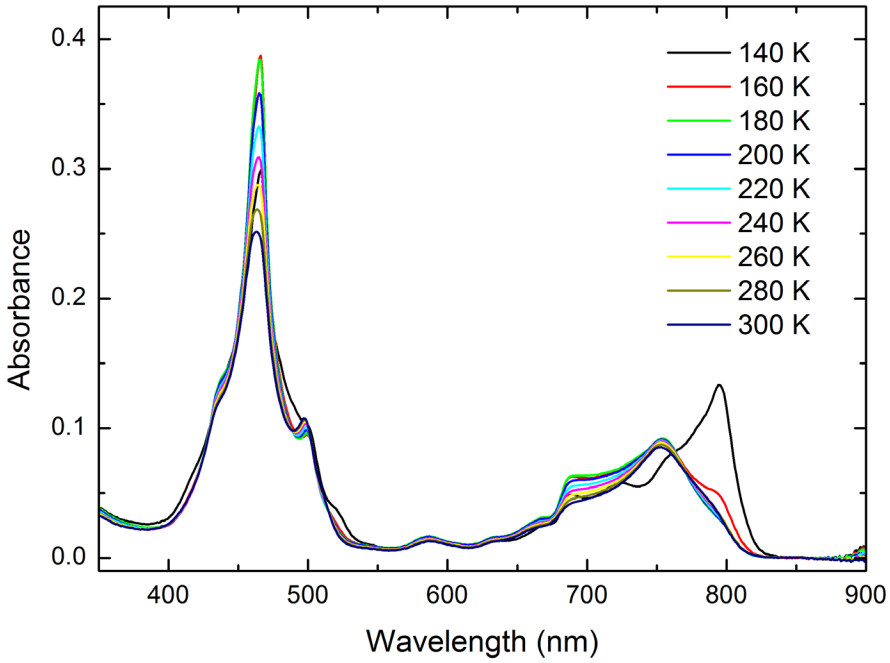

Figure S6.3. Ground state absorption of **P_3-C_{60}** in 2MTHF + 1% pyridine at different temperatures.

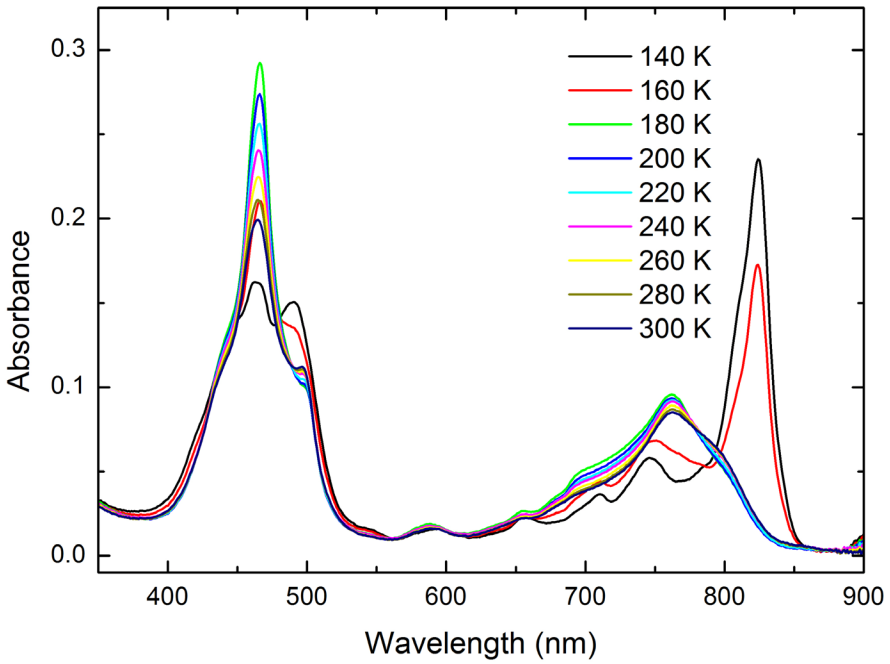

Figure S6.4. Ground state absorption of **P_4-C_{60}** in 2MTHF + 1% pyridine at different temperatures.

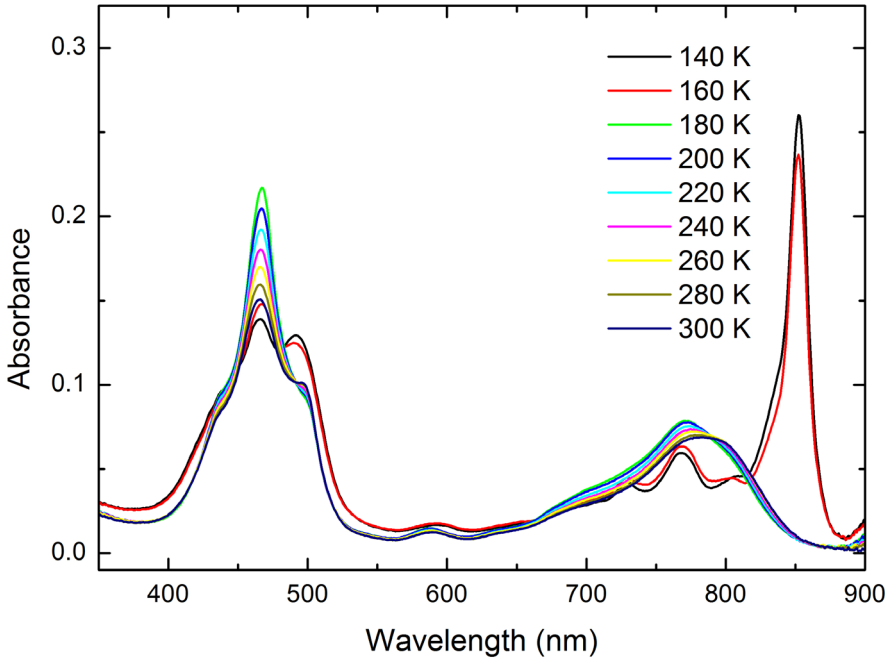

Figure S6.5. Ground state absorption of **P_6-C_{60}** in 2MTHF + 1% pyridine at different temperatures.

Section S7: **Fluorescence spectra of the oligoporphyrin-fullerene compounds at different temperatures**

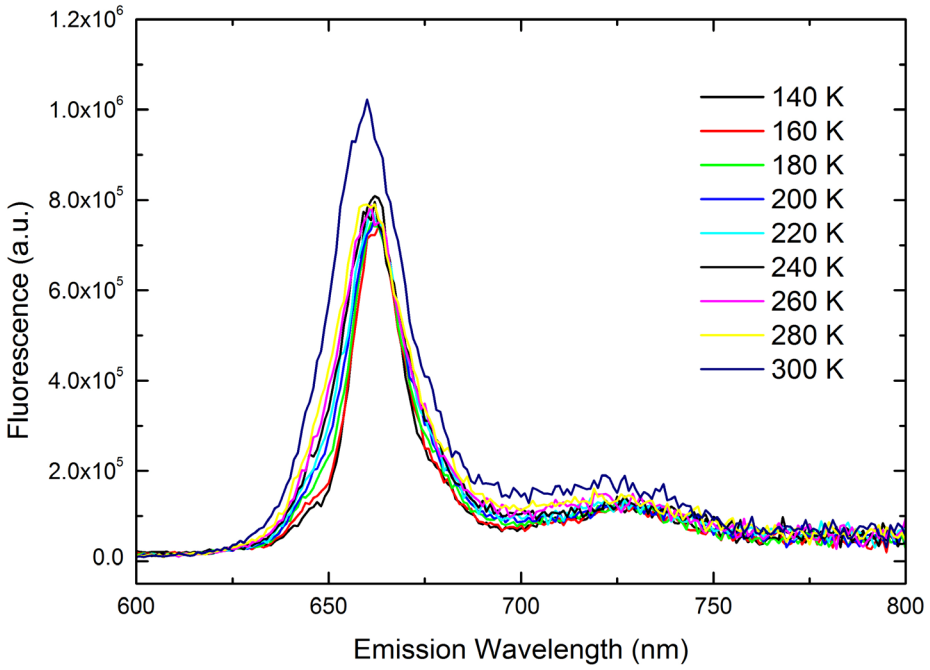

Figure S7.1. Steady state emission of **P_1-C_{60}** in 2MTHF + 1% pyridine at different temperatures excited at 450 nm.

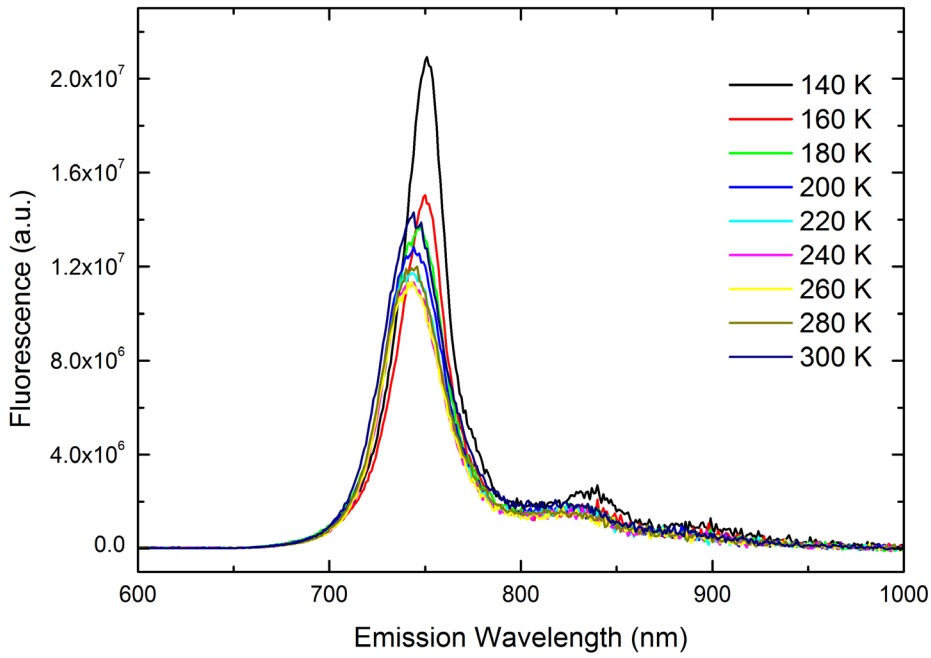

Figure S7.2. Steady state emission of **P_2-C_{60}** in 2MTHF + 1% pyridine at different temperatures, excited at 495 nm.

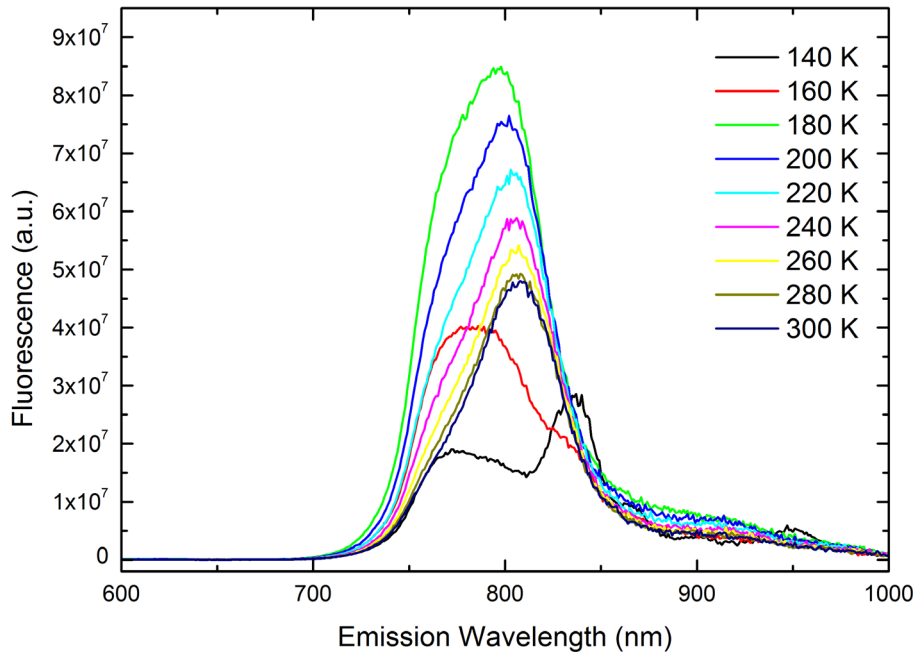

Figure S7.3. Steady state emission of **P_4-C_{60}** in 2MTHF + 1% pyridine at different temperatures excited at 495 nm.

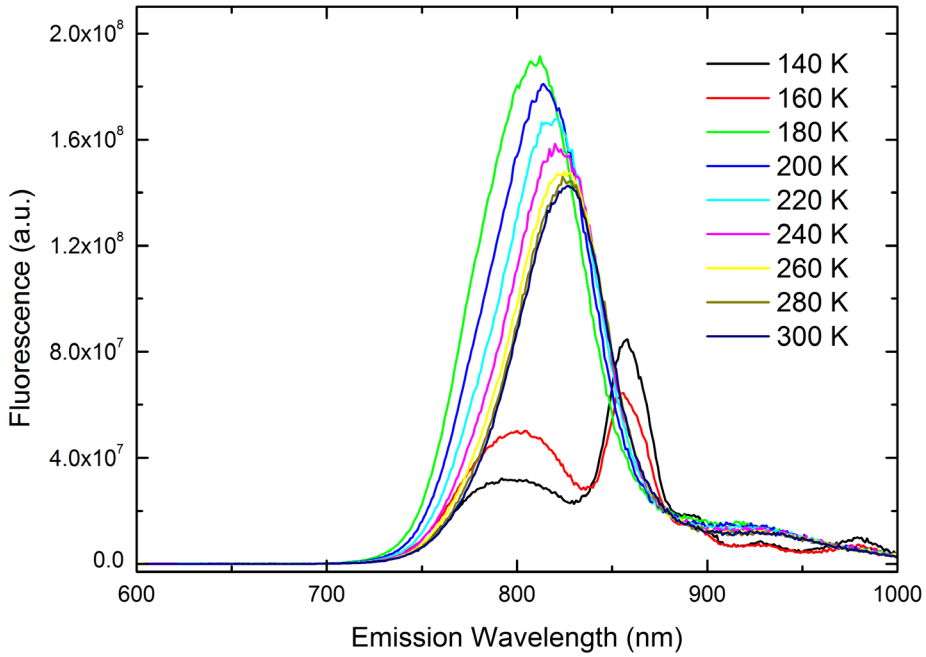

Figure S7.4. Steady state emission of **P_6-C_{60}** in 2MTHF + 1% pyridine at different temperatures excited at 495 nm.

Section S8: **Fluorescence time profiles of the oligoporphyrin-fullerene compounds at different temperatures**

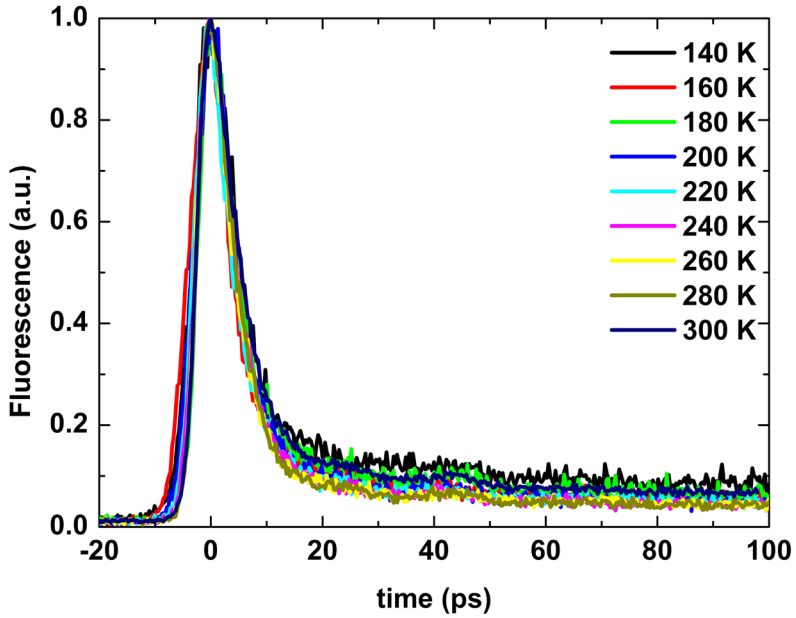

Figure S8.1. Fluorescence time profiles for $\mathbf{P_1}$-$\mathbf{C_{60}}$ in 2MTHF + 1% pyridine at different temperatures.

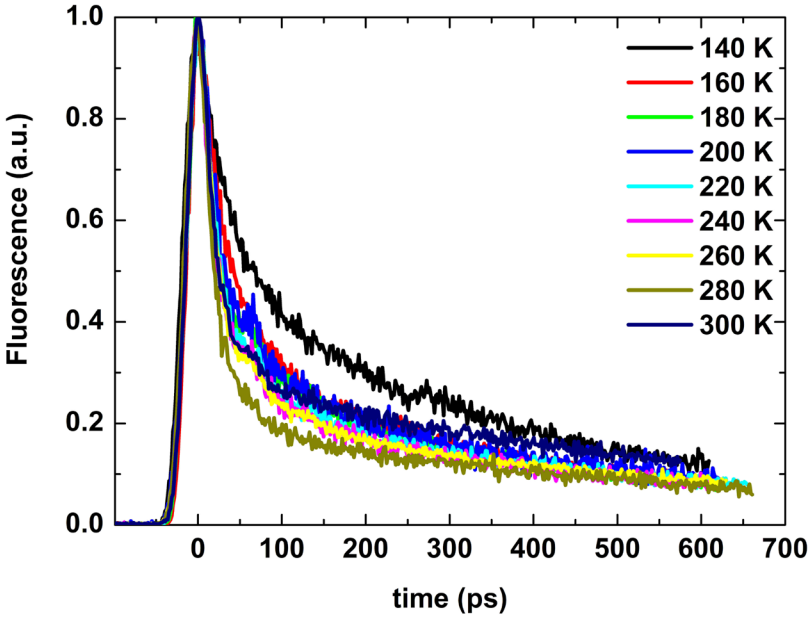

Figure S8.2. Fluorescence time profiles for $\mathbf{P_2}$-$\mathbf{C_{60}}$ in 2MTHF + 1% pyridine at different temperatures.

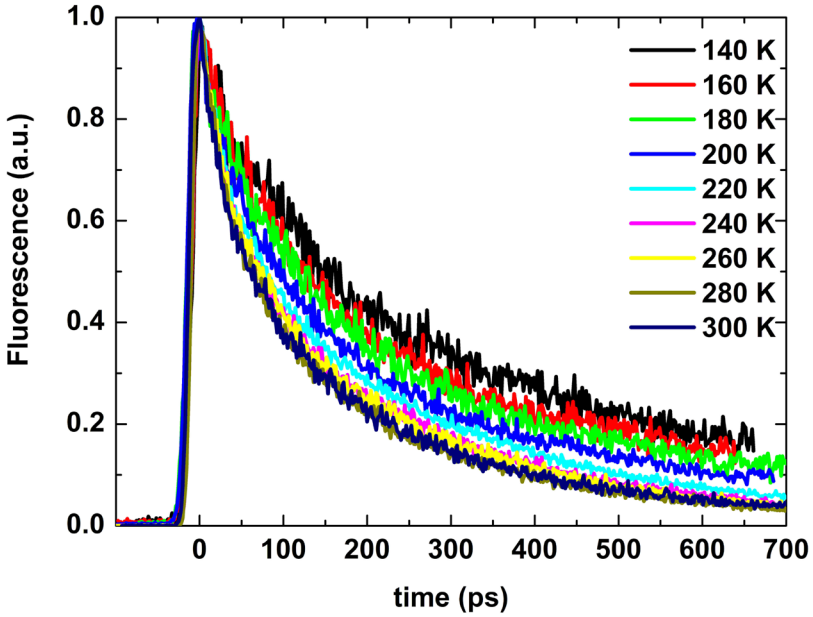

Figure S8.3. Fluorescence time profiles for $\mathbf{P_4}$-$\mathbf{C_{60}}$ in 2MTHF + 1% pyridine at different temperatures.

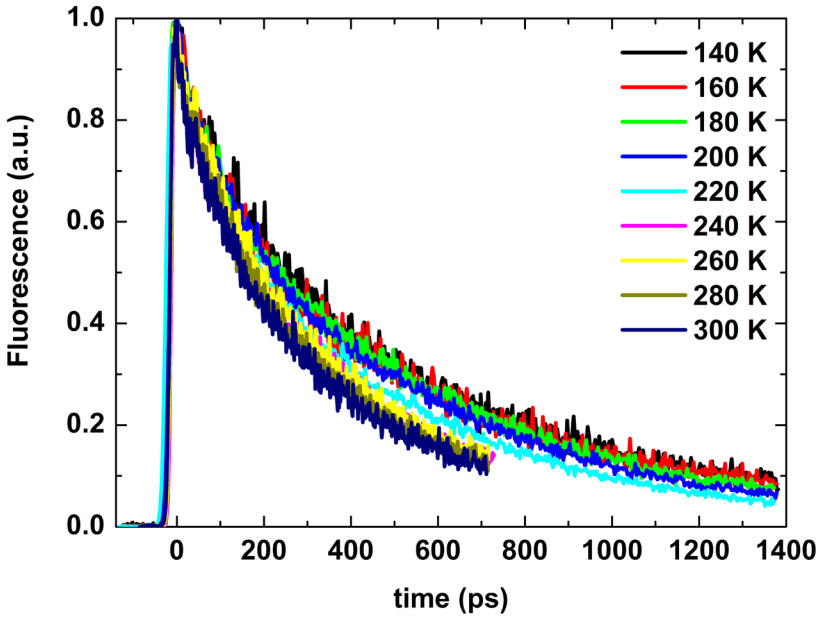

Figure S8.4. Fluorescence time profiles for $\mathbf{P_6}$-$\mathbf{C_{60}}$ in 2MTHF + 1% pyridine at different temperatures.

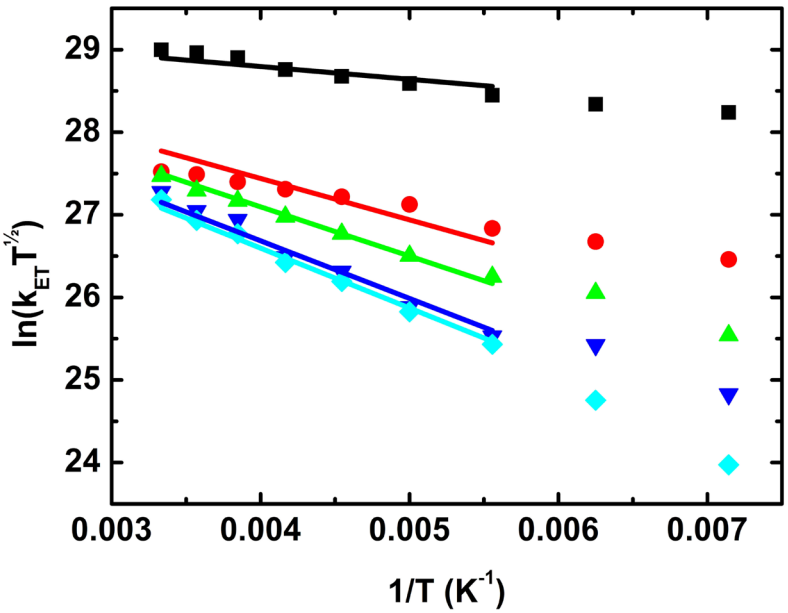

Figure S8.5. Rate constants for charge separation plotted against 1/T (**P**$_1$-**C**$_{60}$ (black), **P**$_2$-**C**$_{60}$ (red), **P**$_3$-**C**$_{60}$ (green), **P**$_4$-**C**$_{60}$ (blue) and **P**$_6$-**C**$_{60}$ (cyan)). The lines are the global fit to the linearized form of Eq.2 assuming a global matrix coupling element V.

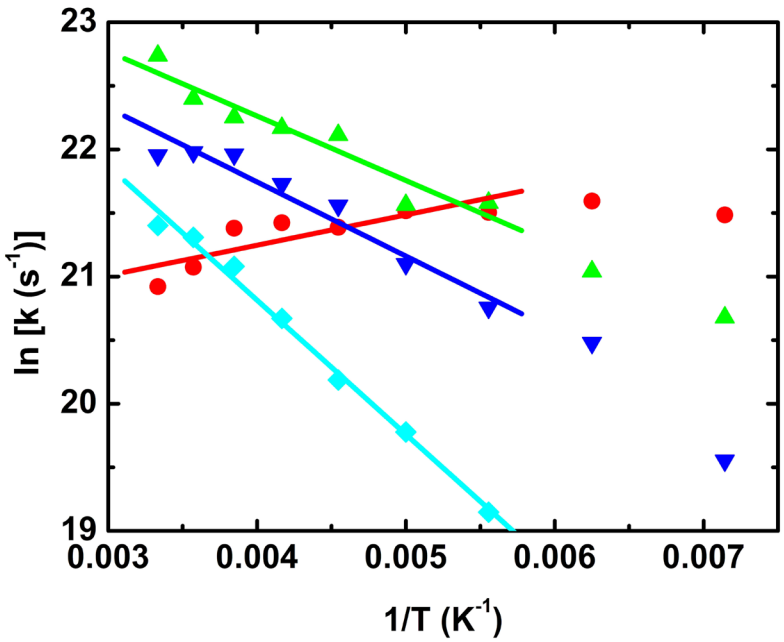

Figure S8.6. Rate constants for excitation energy migration plotted against 1/T, **P**$_2$-**C**$_{60}$ (red), **P**$_3$-**C**$_{60}$ (green), **P**$_4$-**C**$_{60}$ (blue) and **P**$_6$-**C**$_{60}$ (cyan)). The activation energies estimated from the slopes are: **P**$_3$-**C**$_{60}$ = 1.01 kcal/mol, **P**$_4$-**C**$_{60}$ = 1.16 kcal/mol and **P**$_6$-**C**$_{60}$ = 2.11 kcal/mol.

Table 8.1. Temperature dependence of the fitted lifetimes for **P_2-C_{60}**, **P_3-C_{60}**, **P_4-C_{60}**, and **P_6-C_{60}** excited at 495 nm, including the normalized pre-exponential factors.

T / K	**P_2-C_{60}**				**P_3-C_{60}**			
	α_1	τ_1 / ps	α_2	τ_2 / ps	α_1	τ_1 / ps	α_2	τ_2 / ps
140	0.59	37	0.41	337	0.47	88	0.53	536
160	0.71	32	0.29	311	0.54	58	0.46	438
180	0.74	29	0.26	332	0.60	51	0.40	306
200	0.76	23	0.24	329	0.68	42	0.32	310
220	0.80	22	0.20	361	0.62	35	0.38	203
240	0.81	21	0.18	352	0.63	29	0.37	194
260	0.83	20	0.17	363	0.66	25	0.34	181
280	0.88	19	0.12	445	0.68	23	0.32	160
300	0.81	19	0.19	489	0.69	20	0.30	119

T / K	**P_4-C_{60}**				**P_6-C_{60}**			
	α_1	τ_1 / ps	α_2	τ_2 / ps	α_1	τ_1 / ps	α_2	τ_2 / ps
140	0.59	158	0.41	660	0.43	269	0.57	707
160	0.57	101	0.43	503	0.37	167	0.63	650
180	0.56	97	0.44	447	0.29	102	0.71	573
200	0.54	74	0.46	376	0.28	76	0.72	519
220	0.47	52	0.53	285	0.34	57	0.66	471
240	0.49	46	0.51	254	0.25	48	0.75	402
260	0.45	31	0.55	215	0.22	36	0.78	337
280	0.51	29	0.49	212	0.26	32	0.74	300
300	0.52	24	0.48	216	0.23	26	0.77	285

Section S9: **Tables of the fitting parameters of the time absorption profiles of the oligoporphyrin-fullerene compounds at different temperatures**

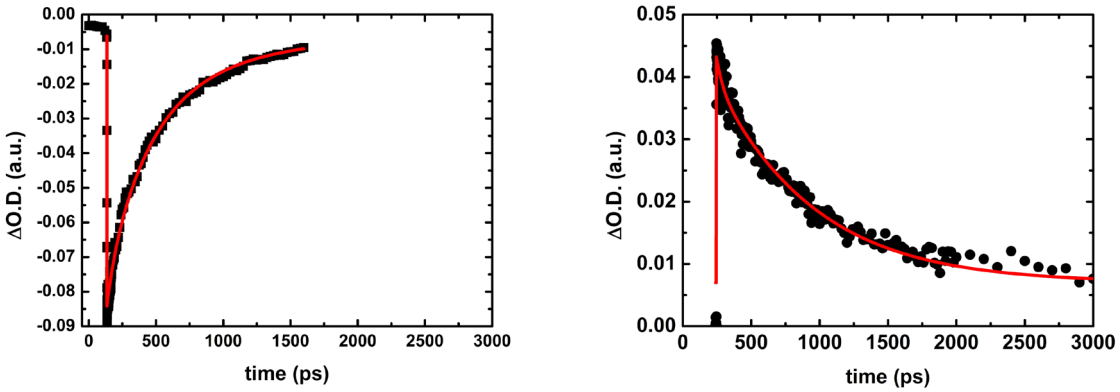

Figure S9.1. Time absorption profiles of $\mathbf{P_4}$-$\mathbf{C_{60}}$ at 220 K. **Left**: Time absorption profile at 730 nm showing the recovery of the Q-band absorption. **Right**: Transient absorption decay at 1015 nm where the $\mathbf{C_{60}}^{\bullet-}$ and $\mathbf{P_4}^{\bullet+}$ species dominate the absorption. The red solid lines show typical fits using the parameters stated in tables 8.4a and 8.4b.

Table S9.1. Fitting parameter for the transient absorption time profiles for $\mathbf{P_1}$-$\mathbf{C_{60}}$ taken at 650 nm representing recovery of the Q-band bleaching.

T / K	α_1	τ_1 / ps	α_2	τ_2 / ps	I_0
140	-0.04681	6.4	-0.03306	455	-0.03113
160	-0.00716	6.2	-0.00750	349	-0.00204
180	-0.00510	5.9	-0.00632	309	-0.00155
200	-0.02348	5.4	-0.03191	274	-0.01371
220	-0.02646	5.2	-0.03316	226	-0.01363
240	-0.00723	5.0	-0.01295	208	-0.00307
260	-0.01760	4.5	-0.03571	201	-0.01912
280	-0.00901	4.4	-0.01636	191	-0.00969
300	-0.00452	4.4	-0.02172	189	-0.01213

Table S9.2a. Fitting parameter for the transient absorption time profiles for $\mathbf{P_2\text{-}C_{60}}$ taken at 720 nm representing recovery of the Q-band bleaching.

T / K	α_1	τ_1 / ps	α_2	τ_2 / ps	α_3	τ_3 / ps	I_0
140	-0.0077	37	-0.0006	337	-0.02671	732	-0.00153
160	-0.00933	32	-0.00051	311	-0.0434	692	-0.00459
180	-0.03533	29	-0.00094	332	-0.03727	640	-0.00576
200	-0.00919	23	-0.00013	329	-0.00516	584	-0.00021
220	-0.02531	22	-0.00127	361	-0.06235	493	-0.00912
240	-0.01408	21	-0.00087	352	-0.02113	454	-0.00283
260	-0.01205	20	-0.00097	363	-0.03214	373	-0.0047
280	-0.00401	19	-0.00177	445	-0.04834	290	-0.00911
300	-0.00306	19	-0.00020	489	-0.02061	276	-0.0005

Table S9.2b. Fitting parameter for the transient absorption time profiles for $\mathbf{P_2\text{-}C_{60}}$ taken at 1015 nm.

T / K	α_1	τ_1 / ps	α_2	τ_2 / ps	α_3	τ_3 / ps	I_0
140	0.00076	37	-0.00048	337	0.00481	732	0.00067
160	0.00196	32	-0.00092	311	0.00551	692	0.00053
180	0.00181	29	-0.00051	332	0.00537	640	0.00016
200	0.00271	23	-0.00024	329	0.00305	584	0.00043
220	0.00159	22	-0.00032	361	0.00371	493	0.00058
240	0.00212	21	-0.00012	352	0.00321	454	0.00032
260	0.00102	20	-0.00071	363	0.00416	373	0.00010
280	0.00212	19	-0.00097	445	0.00558	290	0.00059
300	0.00108	19	-0.00031	489	0.00449	276	0.00071

Table S9.3a. Fitting parameter for the transient absorption time profiles for $\mathbf{P_3\text{-}C_{60}}$ taken at 730 nm representing recovery of the Q-band bleaching.

T / K	α_1	τ_1 / ps	α_2	τ_2 / ps	α_3	τ_3 / ps	I_0
140	-0.0043	88	-0.01373	536	-0.00066	904	-0.012
160	-0.01715	58	-0.01073	438	-0.0105	794	-0.025
180	-0.00119	51	-0.0048	306	-0.06186	710	-0.0216
200	-0.02776	42	-0.02335	310	-0.03643	696	-0.026
220	-0.01525	35	-0.01774	203	-0.0529	627	-0.021
240	-0.02092	29	-0.03724	194	-0.0212	554	-0.031
260	-0.04388	25	-0.04044	181	-0.04029	504	-0.027
280	-0.00845	23	-0.01275	160	-0.06033	483	-0.0162
300	-0.00503	20	-0.00076	119	-0.08282	463	-0.02571

Table S9.3b. Fitting parameter for the transient absorption time profiles for $\mathbf{P_3\text{-}C_{60}}$ taken at 1015 nm.

T / K	α_1	τ_1 / ps	α_2	τ_2 / ps	α_3	τ_3 / ps	I_0
140	0.00105	88	-0.00126	536	0.00668	904	0.0010
160	0.00071	58	-0.00065	438	0.00455	794	0.0005
180	0.00088	51	-0.00199	306	0.00769	710	0.0010
200	0.00075	42	-0.00201	310	0.01161	696	0.0010
220	0.00038	35	-0.00147	203	0.00989	627	0.00075
240	0.00046	29	-0.00192	194	0.00952	554	0.00065
260	0.00266	25	-0.00480	181	0.01259	504	0.00064
280	0.00552	23	-0.00212	160	0.02051	483	0.002
300	0.00012	20	-0.00022	119	0.00332	463	0.001

Table S9.4a. Fitting parameter for the transient absorption time profiles for **P_4-C_{60}** taken at 750 nm representing recovery of the Q-band bleaching.

T / K	α_1	τ_1 / ps	α_2	τ_2 / ps	α_3	τ_3 / ps	I_0
140	-0.0035	158	-0.00122	660	-0.0127	917	-0.0045
160	-0.00781	101	-0.01178	503	-0.00554	846	-0.0079
180	-0.01337	97	-0.00181	447	-0.01908	734	-0.0097
200	-0.02109	74	-0.00766	376	-0.03657	708	-0.0050
220	-0.00697	52	-0.04257	285	-0.0285	689	-0.0062
240	-0.02319	46	-0.01182	254	-0.02293	604	-0.0019
260	-0.02999	31	-0.01972	215	-0.01231	567	-0.0012
280	-0.01143	29	-0.01096	212	-0.01101	538	-0.0017
300	-0.00207	24	-0.00319	216	-0.03318	499	-0.0021

Table S9.4b. Fitting parameter for the transient absorption time profiles for **P_4-C_{60}** taken at 1015 nm.

T / K	α_1	τ_1 / ps	α_2	τ_2 / ps	α_3	τ_3 / ps	I_0
140	0.01638	158	-0.00918	660	0.03414	917	0.0020
160	0.00902	101	-0.00814	503	0.04898	846	0.0054
180	0.00355	97	-0.00091	447	0.0354	734	0.0075
200	0.00293	74	-0.00419	376	0.03192	708	0.0085
220	0.00472	52	-0.00269	285	0.03421	689	0.0070
240	0.00142	46	-0.00582	254	0.03859	604	0.0071
260	0.00045	31	-0.00041	215	0.01273	567	0.00255
280	0.00034	29	-0.02201	212	0.11566	538	0.01154
300	0.00939	24	-0.04715	216	0.14728	499	0.00972

Table S9.5a. Fitting parameter for the transient absorption time profiles for $\mathbf{P_6\text{-}C_{60}}$ taken at 785 nm representing recovery of the Q-band bleaching.

T / K	α_1	τ_1 / ps	α_2	τ_2 / ps	α_3	τ_3 / ps	I_0
140	-0.00514	269	-0.00245	707	-0.00194	1112	-0.001
160	-0.00107	167	-0.00139	650	-0.00188	1005	-0.003
180	-0.00593	102	-0.00724	573	-0.00392	951	-0.0044
200	-0.00334	76	-0.00471	519	-0.00556	903	-0.0035
220	-0.00588	57	-0.00651	471	-0.0071	821	-0.0095
240	-0.00528	48	-0.00525	402	-0.00349	786	-0.0165
260	-0.00302	36	-0.0032	337	-0.00498	748	-0.0058
280	-0.00482	32	-0.00383	300	-0.00372	658	-0.005
300	-0.00177	26	-0.00446	285	-0.00342	643	-0.0031

Table S9.5b. Fitting parameter for the transient absorption time profiles for $\mathbf{P_6\text{-}C_{60}}$ taken at 1015 nm.

T / K	α_1	τ_1 / ps	α_2	τ_2 / ps	α_3	τ_3 / ps	I_0
140	0.00316	269	0.00075	707	0.00315	1112	0.0007
160	0.00621	167	0.09045	650	0.04249	1005	0.00947
180	0.00068	102	0.01503	573	0.00182	951	0.00191
200	0.00145	76	0.00618	519	0.00449	903	0.00081
220	0.00072	57	0.00587	471	0.0126	821	0.00108
240	0.00060	48	0.00334	402	0.01125	786	0.00145
260	0.00089	36	0.00199	337	0.01373	748	0.00108
280	0.00044	32	0.00141	300	0.01801	658	0.0016
300	0.00088	26	0.00247	285	0.0148	643	0.00177

References

(1) Winters, M. U.; Dahlstedt, E.; Blades, H. E.; Wilson, C. J.; Frampton, M. J.; Anderson, H. L.; Albinsson, B. *J. Am. Chem. Soc.* **2007**, *129*, 4291-4297.

(2) Hoffmann, M.; Karnbratt, J.; Chang, M. H.; Herz, L. M.; Albinsson, B.; Anderson, H. L. *Angew. Chem. Int. Ed.* **2008**, *47*, 4993-4996.

(3) Rio, Y.; Accorsi, G.; Nierengarten, H.; Rehspringer, J.-L.; Honerlage, B.; Kopitkovas, G.; Chugreev, A.; Dorsselaer, A. V.; Armaroli, N.; Nierengarten, J.-F. *New J. Chem.* **2002**, *26*, 1146-1154.

(4) Nielsen, C. B.; Johnsen, M.; Arnbjerg, J.; Pittelkow, M.; McIlroy, S. P.; Ogilby, P. R.; Jørgensen, M. *J. Org. Chem.* **2005**, *70*, 7065-7079.

(5) Balija, A. M.; Kohman, R. E.; Zimmerman, S. C. *Angew. Chem. Int. Ed.* **2008**, *47*, 8072-8074.

(6) Ajamaa, F.; Figueira Duarte, T. M.; Bourgogne, C.; Holler, M.; Fowler, P. W.; Nierengarten, J.-F. *Eur. J. Org. Chem.* **2005**, *2005*, 3766-3774.